ELSEVIER

Biochimica et Biophysica Acta 1468 (2000) 359–366

BIOCHIMICA ET BIOPHYSICA ACTA
BBA

www.elsevier.com/locate/bba

Comparative dynamics and location of chain spin-labelled sphingomyelin and phosphatidylcholine in dimyristoyl phosphatidylcholine membranes studied by EPR spectroscopy

Peter Hoffmann [a], Konrad Sandhoff [a], Derek Marsh [b,*]

[a] *Institut für Organische Chemie und Biochemie der Rheinischen Friedrich-Wilhelms-Universität, Gerhard-Domagk-Str. 1, D-53121 Bonn, Germany*

[b] *Abteilung Spektroskopie, Max-Planck-Institut für biophysikalische Chemie, Am Faßberg 11, D-37070 Göttingen, Germany*

Received 20 March 2000; received in revised form 9 June 2000; accepted 6 July 2000

Abstract

The dynamics and environment of sphingomyelin spin-labelled at different positions in the *N*-acyl chain have been studied in dimyristoyl phosphatidylcholine bilayer membranes by using electron spin resonance spectroscopy. Comparison was made with phosphatidylcholine spin-labelled on the *sn*-2 acyl chain in the same host membrane. Spin-labelled sphingomyelin was found to mix well with the host phosphatidylcholine lipids in both gel and fluid phase membranes. At 1 mol%, mutual spin–spin interactions are no greater than for spin-labelled phosphatidylcholine. In the fluid membrane phase, the effective chain order parameters and polarity-sensitive isotropic hyperfine coupling constants of spin-labelled sphingomyelin display a similar dependence on the position of labelling to those of spin-labelled phosphatidylcholine. The values of both parameters are, however, generally larger for sphingomyelin than for phosphatidylcholine at equivalent positions of acyl chain labelling. This difference is attributed to the different chain linkage of sphingo- and glycero-lipids, combined with an offset of approximately one C-atom in transbilayer register between the respective *N*-acyl and *O*-acyl chains. In the gel phase, differences in chain configuration between sphingomyelin and phosphatidylcholine are indicated by differences in spin label spectral anisotropy between the two lipids, which appears to reverse towards the terminal methyl chain end.

Keywords: Sphingolipid; Sphingomyelin; Lipid bilayer; Spin label; Electron paramagnetic resonance; Lipid dynamics; Polarity profile

1. Introduction

Interest has recently centred on the functional behaviour of sphingolipids. It has been proposed that sphingolipids form rafts, or microdomains that contain those proteins, specifically glycophosphatidylinositol-linked proteins, that are destined for the apical surface of bipolar epithelial cells [1]. Sphingolipid raft formation was proposed to be the vehicle for protein sorting in polarised cells, and possibly also for plasma membrane sorting in other cell types [2]. The sphingolipid rafts contain cholesterol, but are deficient in glycerolipids which are sorted to the basolateral membrane in bipolar cells.

Abbreviations: EPR, electron paramagnetic resonance; *n*-SMSL, *N*-[*n*-(4,4-dimethyloxazolidine-*N*-oxyl)stearoyl]-sphingosine-1-phosphocholine; *n*-PCSL, 1-acyl-2-(*n*-(4,4-dimethyloxazolidine-*N*-oxyl)stearoyl)-*sn*-glycero-3-phosphocholine; DMPC, 1,2-dimyristoyl-*sn*-glycero-3-phosphocholine

* Corresponding author. Fax: +49-551-201-1501; E-mail: dmarsh@gwdg.de

0005-2736/00/$ – see front matter
PII: S0005-2736(00)00276-5

As a first approach to defining the interactions that may govern sorting of sphingolipids, it is of interest to investigate the comparative properties of a sphingolipid in a fully defined glycerolipid host membrane. Electron paramagnetic resonance (EPR) spectroscopy of different lipid species with specifically spin-labelled chains has proven to be a powerful way of addressing this problem. The relative location and mobility of the corresponding chain segments have been determined for spin-labelled diacylglycerols [3] and for spin-labelled fatty acids [4], each in a phosphatidylcholine host lipid membrane. In these cases, the comparison was calibrated relative to the corresponding spin-labelled phosphatidylcholines. Additionally, broadening of the EPR spectrum by mutual interactions between spin labels can be used to detect separation of the spin-labelled lipid from the host lipids in the membrane, particularly in the gel phase.

In the present work, we have studied sphingomyelins spin-labelled at different positions in the *N*-acyl chain, in bilayer membranes of 1,2-dimyristoyl-*sn*-glycero-3-phosphocholine (DMPC), in both the gel and fluid phases. Sphingomyelin is the sphingolipid with an identical phosphocholine polar headgroup to that of the phosphatidylcholine glycerolipid. The two lipids differ solely in their chain linkage and chain composition. A comparison of the spin-labelled sphingomyelins was made with corresponding phosphatidylcholines spin-labelled in the *sn*-2 acyl chain. In addition to the spectral anisotropy, which is determined by the mobility of the spin-labelled chain segments, the polarity-sensitive isotropic hyperfine coupling constants were determined to locate the vertical position of the spin-labelled chain, relative to the host lipids of the membrane (see e.g. [5]). Spin-labelled sphingomyelin is found to mix well with the DMPC host lipids at probe concentrations, but the sphingolipid *N*-acyl chain is located somewhat differently from the *sn*-2 acyl chains of the host glycerolipid. The segmental mobility of the chain is also different, especially close to the region of chain attachment. These differences may optimise the interactions that can give rise to raft or microdomain formation by sphingolipids at bulk concentrations.

2. Materials and methods

DMPC was obtained from Fluka (Buchs, Switzerland). Stearic acids spin-labelled at C-atom position *n* in the chain (*n*-(4,4-dimethyloxozolidine-*N*-oxyl), *n*-SASL) were synthesised as described in [6], and the corresponding phosphatidylcholines spin-labelled in the *sn*-2 acyl chain (1-acyl-2-(*n*-(4,4-dimethyloxazolidine-*N*-oxyl)stearoyl)-*sn*-glycero-3-phosphocholine (*n*-PCSL)) were synthesised as described also in [6]. Sphingomyelins spin-labelled in the *N*-acyl chain (*N*-[*n*-(4,4-dimethyloxazolidine-*N*-oxyl)stearoyl]-sphingosine-1-phosphocholine (*n*-SMSL)) were synthesised from the corresponding *n*-SASL spin labels as described in [7]. DMPC and 1 mol% of spin-labelled lipid were codissolved in chloroform:methanol (2:1 v/v); the organic solvent was evaporated in a nitrogen gas stream and the samples were then dried under vacuum overnight. The dry spin-labelled lipid was dispersed in excess buffer by vortex mixing at a temperature above the gel-to-fluid transition of hydrated DMPC (23°C). The spin-labelled lipid dispersion was introduced into 1 mm i.d. glass capillaries and concentrated by centrifugation in a bench centrifuge. It should be emphasised that the multilamellar liposomes prepared by this method are fully hydrated and all are sufficiently large that the lipid packing is not strained by membrane curvature.

EPR spectra were recorded on a Varian Century Line 9 GHz spectrometer equipped with nitrogen gas-flow temperature regulation. Sample capillaries were accommodated within standard 4 mm diameter quartz EPR tubes, that contained light silicone oil for thermal stability. The temperature was measured with a fine-wire thermocouple located in the silicone oil just above the top of the microwave cavity.

Apparent order parameters and isotropic ^{14}N-hyperfine coupling constants were calculated, respectively, according to:

$$S^{\mathrm{eff}} = (A_{\parallel} - A_{\perp})/[A_{zz} - 1/2(A_{xx} + A_{yy})]a'_0/a_0 \qquad (1)$$

$$a_0^{\mathrm{eff}} = (1/3)(A_{\parallel} + 2A_{\perp}) \qquad (2)$$

where $A_{\parallel}$ is $A_{\max}$, half of the outer hyperfine splitting, and $A_{\perp}$ is obtained from $A_{\min}$, which is half of the inner hyperfine splitting according to [8,9]:

$$A_{\perp}(G) = A_{\min}(G) + 0.85 \ (S^{\mathrm{eff}} < 0.45)$$

$$A_{\perp}(G) = A_{\min}(G) + 1.32 + 1.86\log(1-S^{\text{eff}})$$

$$(S^{\text{eff}} > 0.45) \quad (3)$$

A_{xx}, A_{yy} and A_{zz} are the principal values of the hyperfine tensor in the nitroxide frame of axes, obtained from measurements in a single crystal environment [10], and:

$$a_0' = (1/3)(A_{xx} + A_{yy} + A_{zz}) \quad (4)$$

is the isotropic hyperfine coupling constant in the single crystal. To minimise slow-motional effects, values of a_0^{eff} (Eq. 2) were obtained from their constant, plateau region at higher temperatures. For spin labels exhibiting isotropic spectra (e.g. 16-PCSL), values of a_0^{eff} were obtained from the baseline crossing points of the first-derivative spectra.

Motions of spin-labelled lipid chains in bilayer membranes are known to contain components in the slow regime of conventional nitroxide EPR spectroscopy [11]. Order parameters defined by the motional narrowing formulation given above are therefore effective values that depend on motional rates as well as amplitudes, at lower temperatures in the fluid phase. Nevertheless, they may be used empirically to compare different spin labels in the same host membrane (see e.g. [3,4]).

3. Results

The EPR spectra of sphingomyelins spin-labelled at different positions in the *N*-acyl chain have been compared with those of corresponding phosphatidylcholines spin-labelled in the *sn*-2 acyl chain. Bilayers of DMPC were used as the host membrane, in the fluid liquid-crystalline phase and also in the ordered gel phase. Both the lipid chain rotational dynamics and the membrane environment of the spin label were probed. This was done by comparing the ^{14}N-hyperfine anisotropy and spectral line splittings of the spin labels that are determined by the segmental chain mobility, and also by comparing the isotropic ^{14}N-hyperfine coupling constants that are sensitive to the environmental polarity in the immediate vicinity of the spin label group (see e.g. [5]).

3.1. EPR spectra of spin-labelled chains

Different positional isomers, *n*, of sphingomyelin spin-labelled in the *N*-acyl chain (i.e. *n*-SMSL) were investigated in bilayer membranes of DMPC. The EPR spectra of the different *n*-SMSL spin labels are compared in Fig. 1 with those of the corresponding positional isomers of phosphatidylcholine, *n*-PCSL, spin-labelled in the *sn*-2 chain. These spectra were recorded at a sample temperature of 32°C, for which hydrated DMPC bilayers are in the fluid phase. The spectra of the sphingomyelin spin labels are qualitatively similar to those of the corresponding phosphatidylcholine spin labels. Both *n*-SMSL

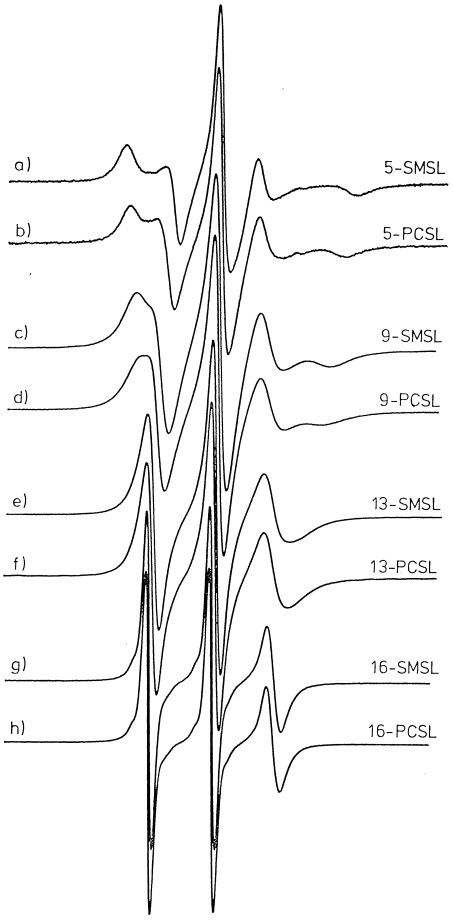

Fig. 1. EPR spectra of *n*-SMSL sphingomyelin spin labels (upper of each pair) and *n*-PCSL phosphatidylcholine spin labels (lower of each pair) in DMPC bilayers at 32°C. The spin label position, *n*, is indicated on the figure. Total scan width = 100 G.

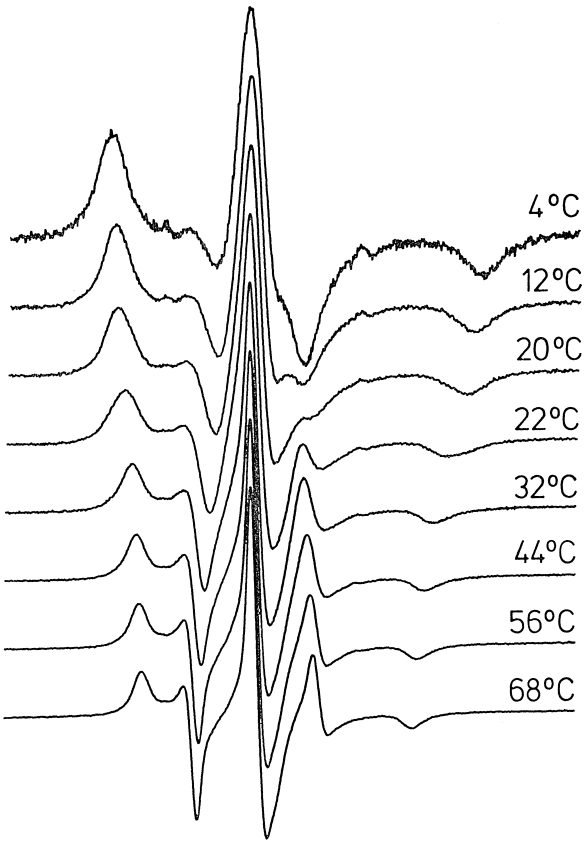

Fig. 2. Temperature dependence of the EPR spectra of the 5-SMSL sphingomyelin spin label in DMPC bilayers. Total scan width = 100 G.

and *n*-PCSL spin labels display axially anisotropic spectra, for which the ^{14}N-hyperfine anisotropy and linewidths decrease with increasing labelling position, *n*, down the lipid chain. This progression corresponds to the chain flexibility profile that is a characteristic feature of fluid, liquid-crystalline lipid membranes. The spectra for a given position of labelling do differ quantitatively, however, between the sphingolipid and glycerolipid chains. This may be attributed to the different backbone linkage of the two types of acyl chains, and possibly also to a resultant offset in vertical register of the sphingomyelin and phosphatidylcholine chains.

3.2. Thermotropic behaviour

The temperature dependence of the EPR spectra of the 5-SMSL sphingomyelin spin label positional isomer in DMPC membranes is given in Fig. 2. The EPR spectrum at low temperature, 4°C in the gel phase, approaches that of a rigidly immobilised powder pattern, on the conventional nitroxide spin-label time scale. Any residual rotational motion of the chain at this position occurs well into the slow-motional regime (rotational correlation times, $\tau_R \approx 10^{-8}$ s). The lack of any appreciable broadening of the spectrum from mutual spin–spin interactions between spin labels indicates, however, that in the gel phase the sphingomyelin component is well mixed with the host phosphatidylcholine membrane lipids, at the spin-label probe concentrations used. With increasing temperature, the spectral lineshapes change slowly in the direction of increasing mobility, in the slow motion regime that applies in the gel phase. At the gel-to-fluid phase transition of the DMPC membranes (ca. 22°C), the spectra change abruptly to those characteristic of a fluid, axially anisotropic, liquid-crystalline phase (cf. Fig. 1). Above this point, the spectral anisotropy decreases gradually with an increase in temperature, corresponding to the gradually increasing chain rotational flexibility.

The temperature dependence of the outer, maxi-

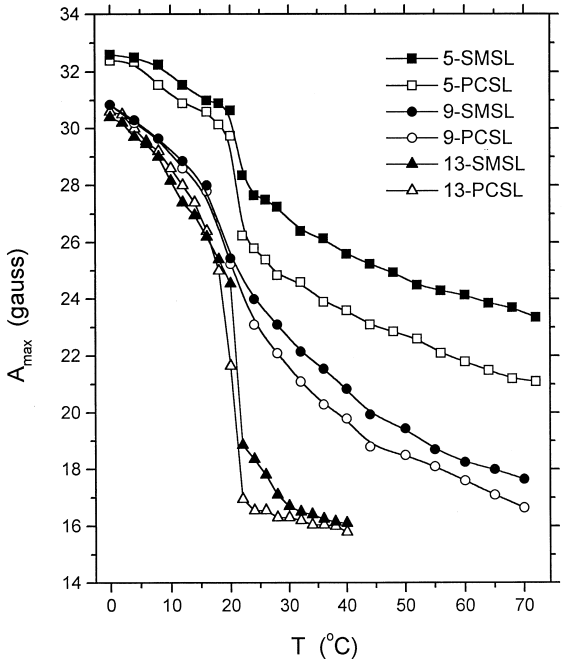

Fig. 3. Temperature dependence of the maximum outer hyperfine splitting, A_{max}, of the *n*-SMSL sphingomyelin spin labels and the *n*-PCSL phosphatidylcholine spin labels in DMPC bilayers.

mum ^{14}N-hyperfine splitting, $2A_{max}$, is given in Fig. 3 for three different positional isomers of both the sphingomyelin spin label, *n*-SMSL, and the phosphatidylcholine spin label, *n*-PCSL. For spin labels at the 5-position, the outer hyperfine splitting constant is close to its maximum, rigid-limit value: $A_{max} = 32.5$ G at 0°C. The outer hyperfine splittings of 5-SMSL and 5-PCSL decrease by a limited amount over the range 10–15°C, corresponding to the pretransition of DMPC bilayers. Then they decrease abruptly, to a much larger extent, at 22°C, corresponding to the chain-melting transition of DMPC bilayers. All three positional isomers display a large decrease in A_{max} at the chain-melting transition, but the spin labels at the 9- and 13-positions display a steeper temperature dependence in the gel phase than do the 5-position spin labels. The spin-labelled sphingomyelin, 5-SMSL, has a somewhat greater value of A_{max} than that of the corresponding 5-PCSL phosphatidylcholine spin label, in the gel phase. For spin labels further down the chain, at the 9- or 13-positions, the difference in splitting between the sphingomyelin and phosphatidylcholine spin labels in gel phase DMPC is much smaller than for those at the 5-position. In fact, the splitting for 13-SMSL is even slightly less than that for 13-PCSL, at low temperature in the gel phase. In fluid DMPC bilayers, however, the values of A_{max} for the sphingomyelin spin labels, *n*-SMSL, are consistently higher than those for the *n*-PCSL phosphatidylcholine spin labels, at all temperatures studied throughout the fluid phase (cf. Fig. 1).

3.3. Chain flexibility gradient

To compare the behaviour of the sphingomyelin spin labels and phosphatidylcholine spin labels more quantitatively in the fluid phase, the effective chain order parameters, S^{eff}, and effective isotropic ^{14}N-hyperfine coupling constants, a_0^{eff}, have been determined as described in Section 2. The positional dependence of the effective order parameters of the *n*-PCSL spin labels in DMPC bilayers at 30°C is given in Fig. 4. Corresponding values from the *n*-SMSL sphingomyelin spin labels are indicated by the horizontal bars on the same figure. These effective values were calculated according to Eqs. 1–4. The effective order parameters of the *n*-PCSL spin labels decrease monotonically with the position, *n*,

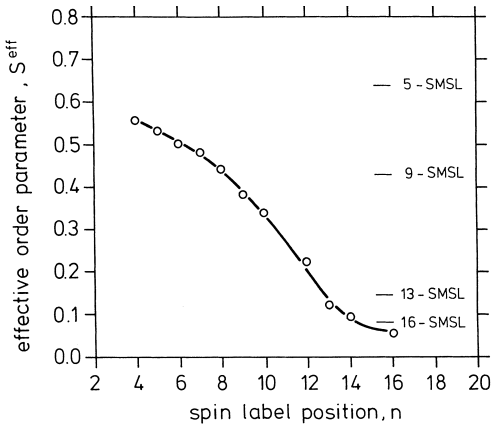

Fig. 4. Profile with chain position, *n*, of the effective order parameter of the *n*-PCSL phosphatidylcholine spin labels in DMPC bilayers at 30°C (○). The effective order parameters, S_{eff}, of the *n*-SMSL sphingomyelin spin labels in DMPC at 30°C are indicated by the horizontal bars.

down the *sn*-2 chain, towards the terminal methyl group. This profile of chain flexibility is a general characteristic of such spin labels in a fluid lamellar phase [12], [13]. The value of S^{eff} for 5-SMSL is greater than that for any of the *n*-PCSL positional isomers studied, at the same temperature. For 9-SMSL, the value of S^{eff} is close to, but somewhat smaller than, that of 8-PCSL. The value of S^{eff} for 13-SMSL is greater than that for 13-PCSL, but substantially smaller than that for 12-PCSL. That for 16-SMSL lies between the values for 14-PCSL and 16-PCSL, but the values for the *n*-PCSL labels are relatively insensitive to *n*, in this region.

3.4. Environmental polarity

The positional dependence of the effective ^{14}N-hyperfine coupling constants of the *n*-PCSL spin labels in DMPC bilayer membranes is given in Fig. 5. Corresponding values for the *n*-SMSL spin labels are given by the horizontal bars, in the same figure. For the lower ranges of *n*, these values were obtained from Eq. 2, in a temperature region for which a_0^{eff} is constant and hence slow-motional contributions to the hyperfine splittings are negligible. For higher values of *n* ($n = 13$–16), the values of a_0^{eff} were measured from the baseline crossing points of isotropic spectra at higher temperatures, again in a region where these values are constant. The dependence of a_0^{eff} on *n* displays the characteristic profile of decreasing polarity

towards the centre of fluid lipid bilayer membranes (see e.g. [5]). The values of a_0^{eff}, and hence of the effective environmental polarity, remain approximately constant for $n=4$ to 6, at the polar headgroup end of the lipid chains. They then decrease abruptly from $n=7$ to 10, to a constant low value that is representative of the apolar middle region of the bilayer membrane. The value of a_0^{eff} for 5-SMSL is somewhat greater than that for any of the *n*-PCSL labels in the region of intermediate polarity, close to the polar–apolar interface. For 9-SMSL, the value of a_0^{eff} is comparable to, but even somewhat larger than, that for the 8-PCSL phosphatidylcholine spin label. The value of a_0^{eff} for 13-SMSL is much lower, and is characteristic of the low polarity region in the middle of the bilayer membrane. That of 16-SMSL is only slightly higher than for 13-SMSL, and is equal to a_0^{eff} for the corresponding 16-PCSL phosphatidylcholine spin label in the same host membrane.

4. Discussion

The characteristic EPR spectra of the *n*-SMSL spin labels indicate that the spin-labelled sphingomyelin mixes well with the host phosphatidylcholine lipids in both gel and fluid phases, at probe concentrations. This allows a direct comparison with the corresponding *n*-PCSL phosphatidylcholines spin-labelled systematically in the *sn*-2 chain. The isotropic hyperfine coupling constants, a_0^{eff}, depend only on the polarity of the environment in which the spin label group is situated. Measurements of a_0^{eff} were made at temperatures sufficiently high to ensure no complications from slow-motional effects. From the most sensitive region of the polarity profile ($n=7$, 10; see Fig. 5), it is found that the *N*-acyl chain of spin-labelled sphingomyelin is approximately one CH_2 segment out of register with the corresponding *sn*-2 chain of spin-labelled phosphatidylcholine. The direction of this displacement is such as to bring a given segment of the sphingolipid *N*-acyl chain closer to the membrane surface than the corresponding segment of the glycerolipid *sn*-2 acyl chain. Other positions of chain labelling, with the exception of a slightly higher effective polarity for 5-SMSL, are consistent with this interpretation (see Fig. 5).

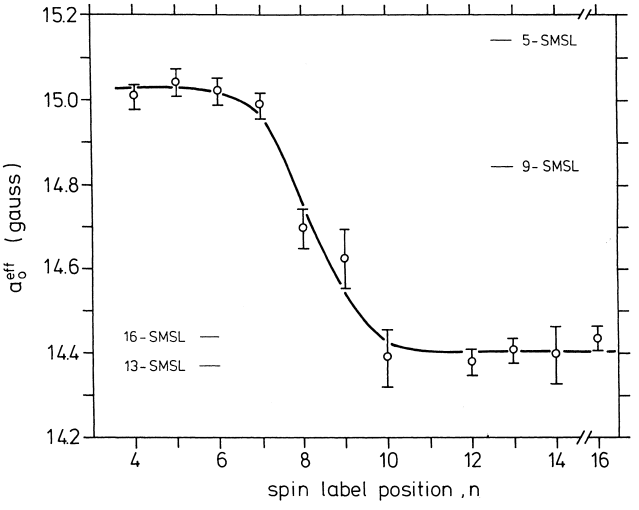

Fig. 5. Profile with chain position, *n*, of the effective isotropic hyperfine splitting constant, a_0^{eff}, of the *n*-PCSL phosphatidylcholine spin labels in DMPC bilayers (○). The effective isotropic splitting constants of the *n*-SMSL sphingomyelin spin labels in DMPC are indicated by the horizontal bars.

The relative displacement of the sphingolipid *N*-acyl chain and glycerolipid *sn*-2 chain is expected to be reflected in the relative segmental flexibility profiles of the two chains in the fluid phase (cf. [3,4]). Examination of Fig. 4 shows this to be qualitatively the case. Quantitatively, however, the effective order parameter for 5-SMSL is considerably greater than even that of 4-PCSL, which suggests that the segmental mobility at this position of labelling is perturbed locally by the specific linkage of the acyl chains in sphingolipids, viz. an amide bond, rather than the ester bond of the *sn*-2 chains in glycerolipids. Coupled with this, as already noted, the environmental polarity of 5-SMSL is somewhat higher than found in the *n*-PCSL glycerolipid series.

In contrast, the segmental mobility near the terminal methyl group of the *n*-SMSL *N*-acyl chain is somewhat higher than might be expected for an upward displacement of one methylene group, relative to the *n*-PCSL phosphatidylcholines. This feature, which is even more pronounced in the gel phase than in the fluid phase, may be attributed to differences in intermolecular packing with the sphingosine chain or *sn*-1 acyl chain, respectively, at the chain ends. In the gel phase, the spectral anisotropy of 13-SMSL (i.e. the value of A_{max}) is actually somewhat smaller than that for 13-PCSL (Fig. 3), which is opposite to the situation for 5-SMSL relative to 5-PCSL.

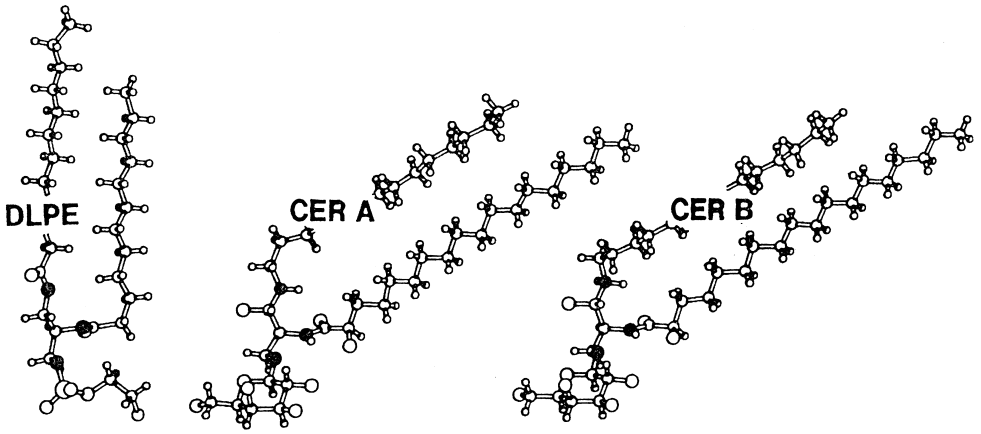

Fig. 6. Backbone conformation (sc/γ/sc) in the crystal structures of glycerolipids and sphingolipids. Left: dilauroyl phosphatidylethanolamine (DLPE); right: galactosyl *N*-hydroxystearoyl cerebroside (CER A, CER B). Adapted from [16] with permission.

This different behaviour of the sphingolipids and glycerolipids with respect to their spin-labelled *N*-acyl and *sn*-2 chains can be explained in terms of the different conformational effects of the chain linkages that are revealed in the crystal structures of the these two classes of lipids (see Fig. 6). Glycerolipids are characterised by a sharp bend in the *sn*-2 chain at the C-2 position that is preserved in the fluid lipid bilayers, as is demonstrated by ^{2}H-NMR studies [14]. Crystal structures are not available for sphingomyelin, but those of cerebrosides may be taken as representative of the sphingolipid class (see Fig. 6). Initially, the sphingosine chain is oriented perpendicular to the bilayer surface. The *N*-acyl chain is attached by an amide link to this section of the sphingosine such that equivalent sections are situated closer to the membrane surface. It is this conformational feature, in addition to the inherent rigidity of the amide unit, that determines much of the difference in dynamic behaviour registered by the *n*-SMSL and *n*-PCSL spin labels. Furthermore, it is seen from Fig. 6 that the *N*-acyl chain of cerebroside extends beyond the end of the sphingosine chain, which is the reverse of the situation for the *sn*-2 chain relative to the *sn*-1 chain in the glycerolipids. This is reflected in the EPR spectra of 13-SMSL, relative to 5-SMSL and 5-PCSL, in the gel phase, as already discussed. Higher segmental mobility is registered by 13-SMSL relative to 13-PCSL because of the lack of intramolecular chain overlap for the former.

In spite of the miscibility of the sphingomyelin spin labels in a phosphatidylcholine host, at probe concentrations, the above differences in chain conformation, mobility and vertical location may contribute to self-association of sphingomyelin at bulk concentrations. Phase separation between different lipids is driven by differences in their intermolecular interactions [15]. The present studies on sphingolipids at probe concentrations indicate a range of configurational differences from the corresponding glycerolipids. It is quite plausible that these rather pronounced differences may contribute directly to the formation of sphingolipid 'rafts' that have been proposed recently as a vehicle for intracellular membrane sorting and a variety of signalling processes [2]. A functional corollary is that bulk membrane domains that are highly enriched in sphingolipids will possess properties that are markedly different from those preferentially enriched in glycerolipids.

Acknowledgements

We thank Frau Brigitta Angerstein for her skillful expertise in preparing spin-labelled lipids.

References

[1] T. Harder, K. Simons, Caveolae, DIGs, and the dynamics of sphingolipid-cholesterol microdomains, Curr. Opin. Cell Biol. 9 (1997) 534–542.
[2] K. Simons, E. Ikonen, Functional rafts in cell membranes, Nature 387 (1997) 569–572.

[3] K. Schorn, D. Marsh, Lipid chain dynamics and molecular location of diacylglycerol in hydrated binary mixtures with phosphatidylcholine: spin label ESR studies, Biochemistry 35 (1996) 3831–3836.
[4] Y.V.S. Rama Krishna, D. Marsh, Spin label ESR and ^{31}P-NMR studies of the cubic and inverted hexagonal phases of dimyristoylphosphatidylcholine/myristic acid (1:2, mol/mol) mixtures, Biochim. Biophys. Acta 1024 (2) (1990) 89–94.
[5] D. Marsh, Electron spin resonance: spin labels, in: E. Grell (Ed.), Membrane Spectroscopy. Molecular Biology, Biochemistry and Biophysics, vol. 31, Springer, Berlin, 1981, pp. 51–142.
[6] D. Marsh, A. Watts, Spin-labeling and lipid–protein interactions in membranes, in: P.C. Jost, O.H. Griffith (Eds.), Lipid–Protein Interactions, vol. 2, Wiley-Interscience, New York, 1982, pp. 53–126.
[7] P. Hoffmann-Bleihauer, Biophysikalische Untersuchungen mit markierten synthetisierten Sphingomyelinen und deren Stoffwechsel am Beispiel verschiedener Modellsysteme, Thesis, University Bonn, Germany, 1986.
[8] W.L. Hubbell, H.M. McConnell, Molecular motion in spin-labelled phospholipids and membranes, J. Am. Chem. Soc. 93 (1971) 314–326.
[9] P.C. Jost, O.H. Griffith, Lipid spin labels in biological membranes, in: L.J. Berliner (Ed.), Spin Labeling. Theory and Applications, Academic Press, New York, 1976, pp. 453–523.
[10] P.C. Jost, L.J. Libertini, V.C. Hebert, O.H. Griffith, Lipid spin labels in lecithin multilayers. A study of motion along fatty acid chains, J. Mol. Biol. 59 (1971) 77–98.
[11] A. Lange, D. Marsh, K.-H. Wassmer, P. Meier, G. Kothe, Electron spin resonance study of phospholipid membranes employing a comprehensive line-shape model, Biochemistry 24 (1985) 4383–4392.
[12] D. Marsh, A. Watts, ESR spin label studies, in: C.G. Knight (Ed.), Liposomes: from Physical Structure to Therapeutic Applications, Elsevier/North-Holland Biomedical Press, Amsterdam, 1981, pp. 139–188.
[13] M. Moser, D. Marsh, P. Meier, K.-H. Wassmer, G. Kothe, Chain configuration and flexibility gradient in phospholipid membranes. Comparison between spin-label electron spin resonance and deuteron nuclear magnetic resonance, and identification of new conformations, Biophys. J. 55 (1989) 111–123.
[14] J. Seelig, A. Seelig, Lipid conformation in model membranes and biological membranes, Q. Rev. Biophys. 13 (1980) 19–61.
[15] G. Cevc, D. Marsh, Phospholipid Bilayers. Physical Principles and Models, Wiley-Interscience, New York, 1987, pp. 1–442.
[16] I. Pascher, M. Lundmark, P.-G. Nyholm, S. Sundells, Crystal structures of membrane lipids, Biochim. Biophys. Acta 1113 (1992) 339–373.